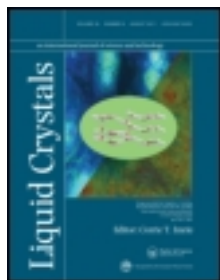


This article was downloaded by: [Jozef Stefan Institute]

On: 16 July 2013, At: 00:19

Publisher: Taylor & Francis

Informa Ltd Registered in England and Wales Registered Number: 1072954 Registered office: Mortimer House, 37-41 Mortimer Street, London W1T 3JH, UK



Liquid Crystals

Publication details, including instructions for authors and subscription information:

<http://www.tandfonline.com/loi/tlct20>

Flow and anchoring effects on nematic fluctuations in confined geometry

Martin Čopič^{a b}, Mojca Vilfan^b & Alenka Mertelj^b

^a Faculty of Mathematics and Physics, University of Ljubljana, Jadranska 19, SI-1000, Ljubljana, Slovenia

^b Joseph Stefan Institute, Jamova 39, SI-1000, Ljubljana, Slovenia

Published online: 12 Jul 2013.

To cite this article: Liquid Crystals (2013): Flow and anchoring effects on nematic fluctuations in confined geometry, Liquid Crystals, DOI: 10.1080/02678292.2013.819129

To link to this article: <http://dx.doi.org/10.1080/02678292.2013.819129>

PLEASE SCROLL DOWN FOR ARTICLE

Taylor & Francis makes every effort to ensure the accuracy of all the information (the "Content") contained in the publications on our platform. However, Taylor & Francis, our agents, and our licensors make no representations or warranties whatsoever as to the accuracy, completeness, or suitability for any purpose of the Content. Any opinions and views expressed in this publication are the opinions and views of the authors, and are not the views of or endorsed by Taylor & Francis. The accuracy of the Content should not be relied upon and should be independently verified with primary sources of information. Taylor and Francis shall not be liable for any losses, actions, claims, proceedings, demands, costs, expenses, damages, and other liabilities whatsoever or howsoever caused arising directly or indirectly in connection with, in relation to or arising out of the use of the Content.

This article may be used for research, teaching, and private study purposes. Any substantial or systematic reproduction, redistribution, reselling, loan, sub-licensing, systematic supply, or distribution in any form to anyone is expressly forbidden. Terms & Conditions of access and use can be found at <http://www.tandfonline.com/page/terms-and-conditions>

Flow and anchoring effects on nematic fluctuations in confined geometry

Martin Čopič^{a,b*}, Mojca Vilfan^b and Alenka Mertelj^b

^aFaculty of Mathematics and Physics, University of Ljubljana, Jadranska 19, SI-1000 Ljubljana, Slovenia; ^bJoseph Stefan Institute, Jamova 39, SI-1000 Ljubljana, Slovenia

(Received 31 May 2013; final version received 20 June 2013)

Light scattering observation of nematic director fluctuations in confined geometries can be used to obtain interaction parameters of liquid crystals with surfaces. We present the basics of the method and some examples of the results in planar and cylindrical geometries. These results were obtained after neglecting the coupling of the director motion to flow. We give analytical and numerical results of flow effects on director fluctuations in a slab. The backflow contribution to the effective viscosity is strongly suppressed so that the results for the anchoring energy remain valid. Modal dispersion relations show an interesting behaviour of avoiding crossings.

Keywords: liquid crystals; nematic fluctuations; light scattering; surface interactions

1. Introduction

Thermally excited director fluctuations are one of the most prominent manifestations of the nematic order in liquid crystals. They make even well-ordered samples appear turbid due to strong scattering of light that is caused by large amplitude of the fluctuations and large optical birefringence. The dynamics of fluctuations in a bulk nematic sample, that is when the wave-length of the fluctuations of interest is much smaller than the dimensions of the sample, are governed by nematic elasticity and viscosity. As the fluctuations are easy to observe by light scattering techniques, they are one of the primary probes of the viscoelastic properties of liquid crystals [1]. By measuring both the intensity of the scattered light and the relaxation rate of the fluctuations that can be obtained from the intensity correlation function of the scattered light, it is in principle possible to obtain all the elastic constants and viscosity parameters of the nematic phase. In practice, due to the difficulties with determination of absolute scattering cross-section, one elastic constant must be obtained by other methods [2–4].

When boundaries are present, the spectrum of the fluctuations must to some extent depend on interactions of the nematic with the surfaces. The most important parameter describing these interactions is surface anchoring energy, usually taken to be of the Rapini–Papoular form [5]. It seems reasonable to assume that the fluctuations would be most strongly affected by surface anchoring close to the surface. So, an early idea of how surface anchoring energy could be obtained by light scattering was investigated by one of the present authors (M.Č.) and Noel Clark on the occasion of a very memorable visit of M.Č. to the University of

Colorado. We analysed the scattering of evanescent wave in a nematic that occurs when light is totally internally reflected in a high-index prism immersed in a nematic liquid crystal [6,7]. Then, evanescent light wave extends into the nematic only in a submicron layer and scattering of this wave is sensitive only to fluctuations in this layer. The result was that while the scattered spectrum does depend on the anchoring energy, the dependence is unspecific and is not very useful to determine the anchoring energy.

The situation is different when nematic liquid crystal is confined, so that at least one dimension is finite, for example in a slab. Light scattering in a thin nematic slab was first theoretically and experimentally examined by Stallinga et al. [8,9]. It was shown that the spectrum of fluctuations is affected by the anchoring energy when the thickness of the slab becomes comparable to the so called extrapolation length that is defined as the ratio of the elastic constant to the surface anchoring strength. We performed a series of experiments in which we showed that the anchoring energy can be very successfully measured by measuring the relaxation time of the fluctuations vs. sample thickness [10–14]. We also showed that it is also possible to obtain the surface viscosity both in planar and cylindrical geometry [15]. This method was later also used by Škarabot et al. [16].

In all this work it was assumed that the effective viscosity governing the relaxation rate of the fluctuations is independent of the sample dimensions. This, however, cannot be entirely correct. The motion of the director is coupled with the shear velocity of the fluid, contributing to the dynamics of the director. This is called the backflow effect. Normally, boundary

*Corresponding author. Email: martin.copic@fmf.uni-lj.si

conditions require that the velocity is zero which should reduce the backflow. In this article, we analyse the fluctuations in a slab with the full equations of the nemato-dynamics and show how this affects the experiments.

The plan of the article is as follows. In Section 2, we will review the simple approach to the dynamics of fluctuations in a slab and the results on anchoring energy obtained by dynamic light scattering. In Section 3, we will present new results of the analysis using the linearised Ericksen–Leslie equations [17–20].

2. Light scattering measurement of anchoring

Nematic fluctuations are overdamped fluctuations of the direction of the nematic order. In the bulk, they are characterised by two polarisations giving two dispersion branches of the relaxation as a function of the wave-vector. The first branch is polarised with the perturbed part \mathbf{n}_1 of the director lying in the plane of the unperturbed director \mathbf{n}_0 and the wave-vector \mathbf{q} . The deformation of the nematic director goes from pure bend for \mathbf{q} parallel to \mathbf{n}_0 to pure splay for \mathbf{q} perpendicular to \mathbf{n}_0 . The second mode polarised perpendicularly to the plane $\mathbf{n}\text{-}\mathbf{q}$ goes from pure bend to pure twist. Their relaxation rates are given by [1].

$$\frac{1}{\tau_i} = \frac{K_i q_{\perp}^2 + K_3 q_z^2}{\eta_i}, \quad i = 1, 2 \quad (1a)$$

$$\eta_1 = \gamma_1 - \frac{(q_{\perp}^2 \alpha_3 - q_z^2 \alpha_2)^2}{q_{\perp}^4 \eta_b + q_{\perp}^2 q_z^2 (\alpha_1 + \alpha_3 + \alpha_4 + \alpha_5) + q_z^4 \eta_c} \quad (1b)$$

$$\eta_2 = \gamma_1 - \frac{q_z^2 \alpha_2}{q_{\perp}^2 \eta_a + q_z^2 \eta_c} \quad (1c)$$

where K_1 , K_2 and K_3 are the splay, bend and twist elastic constants, α_i are Leslie viscosity coefficients, $\gamma_1 = \alpha_3 - \alpha_2$ is pure rotational viscosity and $\eta_a = \alpha_4/2$, $\eta_b = (\alpha_2 + 2\alpha_3 + \alpha_4 + \alpha_5)/2$ and $\eta_c = (-\alpha_2 + \alpha_4 + \alpha_5)/2$ are Miesowicz viscosities. The second term in the Equations (1b,c) describes the effect of flow on the effective viscosity. This backflow contribution is most pronounced for the bend mode and less so for the splay, due to the relative magnitudes of the relevant Leslie coefficients ($|\alpha_2| \gg |\alpha_3|$). The pure twist mode is not coupled to flow. As the Leslie coefficients are known only for very few substances [2,21,22], the dependence of the viscous torque on the direction of \mathbf{q} is often neglected and an effective viscosity is used.

Wave-like excitations in any medium that is limited in one or more dimensions by boundaries, with some boundary conditions are characterised by a

wave-vector only in the unbounded directions, while the bounded dimensions give rise to discrete modes. Except in the case of completely free boundary conditions, even the lowest order mode has a nonzero value for the frequency or relaxation rate at zero wave-vector. This mode is most strongly affected by the boundary conditions and in the case of a nematic slab can be used to determine the anchoring energy.

Let us consider the simple case of planar orientation of a nematic liquid crystal in a slab of thickness $2a$. Let z -axis be perpendicular to the slab with the origin in the middle, and let x -axis be in the direction of \mathbf{n}_0 , the plane of the slab. For now, let us also neglect the coupling of the director and flow. Then, the equation for the motion of the director is simply

$$K_i \frac{\partial^2 n_i}{\partial z^2} = \eta_{eff} \frac{\partial n_i}{\partial t} \quad (2)$$

where $i = 1$ for splay and 2 for twist. Anchoring energy is taken to be of Rapini–Papoular form $W_i \sin^2 \phi_i$, with i denoting either zenithal angle (out-of-plane) for splay fluctuations or azimuthal for twist. For small fluctuations, this energy gives rise to boundary condition

$$K_i \left. \frac{\partial n_i}{\partial z} \right|_{z=\pm a} = \pm W_i \quad (3)$$

The solutions to Equations (2) and (3) are $n_i = A \cos qz \exp(-t/\tau)$ for even modes ($\sin qz$ for odd), with the relaxation rate $1/\tau = K_i q^2 / \eta_{eff}$. From the boundary conditions we get that q must satisfy

$$q \tan qa = \frac{W_i}{K_i} = \frac{1}{\lambda_i} \quad (4)$$

here, λ is the extrapolation length. For the more important case with λ not much smaller than a , a relatively good approximate solution of the transcendental Equation (4) gives the relaxation time of the lowest order mode

$$\tau = \frac{\eta_{eff} a}{W_i} + \frac{\eta_{eff} a^2}{3K_i} \quad (5)$$

This is the basis for the measurement of the anchoring energy using light scattering. It is necessary to obtain the relaxation time of the fundamental mode as a function of the sample thickness $2a$. Then the coefficient of the linear part gives the anchoring energy, provided that either K_i or η_{eff} are known. It is also assumed that η_{eff} does not depend on boundaries.

In the experiments, we prepared samples of 5CB in the form of a wedge with thickness going from 6 μm

to 200 nm. In one case, the orienting layer was rubbed nylon [13], giving planar orientation. By proper choice of scattering geometry, both azimuthal W_2 and zenithal W_1 anchoring coefficients were measured for different rubbing strength. It was found that the anchoring energies are in the range of $5 \times 10^{-6} \text{ J/m}^2$ to $3 \times 10^{-5} \text{ J/m}^2$. Zenithal anchoring was about two times stronger than azimuthal. We also studied the dependence of W_i on temperature [14]. We found that the ratio of the anchoring coefficients is nearly independent of temperature and equal to the ratio of the splay and twist elastic constants. The extrapolation lengths slightly increased close to the transition to the nematic state. This indicates that the observed macroscopic anchoring coefficients, which are essentially defined through extrapolation lengths, result from the following mechanism. Rubbed polymer surface is only partially ordered, as can be deduced from the small optical anisotropy of the polymer layer. So the adsorbed liquid crystal molecules have only a small degree of order at the surface and the bulk order is established by bulk elastic interactions through a layer with thickness of the order of the correlation length of the surface order. It is worth noting that the anchoring energy that would result from fully ordered first adsorbed molecular layer, interacting with the substrate by Van der Waals force, would be of the order of 10^{-2} J/m^2 .

In another experiment, we looked at aging of the anchoring strength of poly-(vinyle-cinnamate) [12]. We found that the anchoring strength increases in the first few days after UV irradiation, probably due to curing. In these samples, we also found that we have to add to the description a surface dissipation term which contributes to the surface torque proportional to the angular velocity of the director at the surface. The boundary conditions then become

$$K_i \left. \frac{\partial n_i}{\partial z} \right|_{z=\pm a} = \pm (W_i + \zeta \dot{n}_i) \quad (6)$$

where ζ is a surface dissipation (viscosity) coefficient. Approximate solution for the relaxation time becomes

$$\tau = \frac{\eta_{ef} a}{W_i} + \frac{\eta_{ef} a^2}{3K_i} + \frac{\zeta}{W_i} \quad (7)$$

We explained this apparent surface viscosity by a thin layer close to the surface that was contaminated by the vinyl-cinnamate monomers. As these cured, ζ decreased with time.

Škarabot et al. used the same method to measure the anchoring strength of 8OCB on DMOAP-silanated glass [16]. This surfactant produces homeotropic anchoring. The obtained value for

the anchoring coefficient was quite high, 10^{-4} J/m^2 , and also nearly independent of temperature.

The above considerations are not limited to planar slab geometry. They similarly apply to cylindrical geometry. We analysed the dynamics of fluctuations by light scattering in 5CB in cylindrical pores in polycarbonate membranes [11,15]. The pore diameters were from 25 nm to 400 nm. The anchoring coefficient was in the range from $3 \times 10^{-6} \text{ J/m}^2$ close to the isotropic transition to $5 \times 10^{-5} \text{ J/m}^2$ at room temperature. We also found a surface dissipation coefficient. The ratio ζ/η_{ef} was of the order of molecular length, indicating that the surface viscosity in this case could be due to increased dissipation caused by dangling ends of the polycarbonate chains at the walls of the pores.

The above examples show the advantage of using light scattering to analyse the interaction of liquid crystals with surfaces. The most demanding part of the measurement is to prepare samples with known varying thickness that is comparable to the extrapolation length. Then, one can obtain reliable values for the anchoring properties of the surface, with little additional effort. Both, in-plane and out-of-plane coefficients can be measured in the same set-up. The method is also applicable in systems that cannot be studied by other methods, like in submicron pores or droplets.

3. Coupling to flow

In the analysis of fluctuations in confined geometries, the coupling of the director motion to the fluid velocity gradients has been neglected. As evident from Equation (1), this coupling changes the effective viscosity and dependence of the relaxation rate on the direction of the wave-vector. One expects that in a finite geometry, the flow is reduced due to the condition that the velocity at the boundaries must be zero. So, it is necessary to find the properties of the fluctuation modes in a confined geometry, especially for the case of a slab as this is used to determine the anchoring energy.

We start from linearised Ericksen–Leslie equations. Like in the bulk, the fluctuation modes have two branches – the bend-splay and the bend-twist one. Let us restrict the analysis to the more interesting case of the bend-splay mode and start with the homeotropic orientation so that the fluctuation that is homogeneous in the plane of the slab is a pure bend. As before, let the z -axis be normal to the slab and x in the plane of the slab. We put the origin in the middle of the slab with thickness $2a$. Then, the fluctuating component of the director is n_x and the relevant velocity components v_x and v_z . Then, the linearised form of the Ericksen–Leslie equations is

$$\gamma_1 \left[\dot{n}_x - \frac{1}{2} \left(\frac{\partial v_z}{\partial x} + \frac{\partial v_x}{\partial z} \right) \right] = K_1 \frac{\partial^2 n_x}{\partial x^2} \quad (8a)$$

$$+ K_3 \frac{\partial^2 n_x}{\partial z^2} - \frac{1}{2} (\alpha_2 + \alpha_3) \left(\frac{\partial v_z}{\partial x} + \frac{\partial v_x}{\partial z} \right) - \frac{\partial p}{\partial x} + \alpha_2 \frac{\partial \dot{n}_x}{\partial z} + \eta_3 \frac{\partial^2 v_x}{\partial z^2} \quad (8b)$$

$$+ \frac{1}{2} (\alpha_2 + \alpha_4 + \alpha_5) \frac{\partial^2 v_z}{\partial x \partial z} + \alpha_4 \frac{\partial^2 v_x}{\partial x^2} = 0$$

$$- \frac{\partial p}{\partial z} + \alpha_3 \frac{\partial \dot{n}_x}{\partial x} + \frac{1}{2} (\alpha_2 + 2\alpha_3 + \alpha_4 + \alpha_5) \frac{\partial^2 v_z}{\partial x^2} + \frac{1}{2} (\alpha_2 + \alpha_4 + \alpha_5) \frac{\partial^2 v_x}{\partial x \partial z} \quad (8c)$$

$$+ (\alpha_1 + \alpha_2 + \alpha_3 + \alpha_4 + 2\alpha_5) \frac{\partial^2 v_z}{\partial z^2} = 0 \quad (8d)$$

$$\nabla \cdot \mathbf{v} = 0.$$

The first equation is the balance of torques, the second two are what remains of the momentum balance after neglecting inertia and linearisation and the last equation is the incompressibility condition which also requires that the pressure is included in the equations. K_1 is the splay and K_3 is the bend elastic constant, and α_i are the five Leslie coefficients. The Parodi relation $\alpha_6 = \alpha_2 + \alpha_3 + \alpha_5$ has been used [23]. The pure rotational viscosity satisfies $\gamma_1 = \alpha_3 - \alpha_2 > 0$ as $\alpha_2 < 0$. We also introduce the combination $\eta_{13} = (\alpha_1 + \alpha_3 + \alpha_4 + \alpha_5)$. In addition to Equations (8), we also have the boundary conditions that $v(x, \pm a) = 0$ and $n_x(x, \pm a) = 0$.

Let us first look at the fluctuations homogeneous in the plane of the slab. Then, $v_z = 0$ everywhere, and n_x and v_x are functions of z only. Pressure can be taken to be constant. Then, the resulting equations are

$$\gamma_1 \dot{n}_x = K_3 \frac{\partial^2 n_x}{\partial z^2} - \alpha_2 v_x \quad (9a)$$

$$\alpha_2 \frac{\partial \dot{n}_x}{\partial z} + \eta_c \frac{\partial^2 v_x}{\partial z^2} = 0 \quad (9b)$$

$$n_x(a) = 0 \quad v_x(a) = 0 \quad (9c)$$

The time dependence must be exponentially decaying with a rate $1/\tau$. Equation (9) can be integrated and give

$$n_x = A (\cos qz - \cos qa) \quad (10a)$$

$$v_x = A \frac{\gamma_1}{\alpha_2 \tau} \left(\frac{\alpha_2^2}{\gamma_1 \eta_c} \frac{1}{q} \sin qz - z \cos qa \right) \quad (10b)$$

The relaxation rate is given by the relation

$$\frac{1}{\tau} \left(\gamma_1 - \frac{\alpha_2^2}{\eta_c} \right) = K_3 q^2 \quad (11)$$

and the transverse wave-number q must satisfy the transcendental equation

$$\beta \tan qa = qa \quad \text{with} \quad \beta = \frac{\alpha_2^2}{\eta_c \gamma_1} \quad (12)$$

Parameter β must be smaller than 1 and is for known cases more than 0.5. For this range, a very good approximate solution is

$$q^2 = \frac{5}{6 - \beta} (1 - \beta) \frac{3}{a^2} \quad (13)$$

giving the relaxation rate

$$\frac{1}{\tau} = \frac{5}{6 - \beta} \frac{3}{a^2} \frac{K_3}{\gamma_1} \quad (14)$$

Equation (14) is close to the result completely neglecting the coupling to flow

$$\frac{1}{\tau} = \frac{K_3}{\gamma_1} \left(\frac{\pi}{2a} \right)^2$$

So, we see that for the pure bend fluctuation, the backflow is strongly reduced, but not completely absent.

Higher order roots of Equation (12), giving q for even modes, and of corresponding equation for odd modes rapidly tend to $n\pi/(2a)$, so that according to Equation (11) the relaxation rate becomes equal to the bulk one.

Next, we look at the dispersion of the mode relaxation rate for finite wave-number in the plane q_x . All the variables are of the form $n_x = e^{-t/\tau} e^{iq_x x} n_x(z)$. We can eliminate pressure and v_x from Equation (11) to arrive at the system of equations

$$\frac{i}{\tau} (\alpha_3 q_x^3 n_x + \alpha_2 n_x'') + \eta_b q_x^4 v_z - \eta_{13} q_x^2 v_z'' + \eta_3 v_z^{IV} = 0 \quad (15a)$$

$$q_x \left(\frac{\gamma_1}{\tau} - K_1 q_x^2 \right) n_x + K_3 q_x n_x'' - i\alpha_3 q_x^2 v_z - i\alpha_2 v_z'' = 0 \quad (15b)$$

with boundary conditions $n_x(a) = 0$, $v_z(a) = 0$ and $v_z'(a) = 0$.

The solution for the fundamental mode is even in z and can be taken in the form

$$\begin{bmatrix} n_x \\ v_z \end{bmatrix} = \sum_{i=1}^3 \begin{bmatrix} A_i \\ B_i \end{bmatrix} \cos q_i z \quad (16)$$

q_i^2 are roots of a third degree polynomial resulting from the determinant of the system (15). They depend on the still unknown τ . To satisfy the boundary conditions we get the determinant

$$\begin{vmatrix} A_i \cos q_i a \\ B_i \cos q_i a \\ -B_i q_i \sin q_i a \end{vmatrix} = 0 \quad i = 1, 2, 3 \quad (17)$$

This is a transcendental equation for τ at given values for the three roots q_i . The solutions to Equations (16) and (17) can be found numerically by expressing the coefficients of the characteristic polynomial in terms of roots, for example $c_2/c_3 = -(q_1^2 + q_2^2 + q_3^2)$, and then solving the resulting system of four nonlinear equations for q_i^2 and τ .

To present the results, we choose values for the parameters that would be expected in a typical material. We set the bend elastic constant K_3 and rotational viscosity γ_1 to be 1. Then, $K_1 = 1.5$, $\alpha_1 = -0.08$, $\alpha_2 = -1.04$, $\alpha_3 = -0.04$, $\alpha_4 = 0.92$ and $\alpha_5 = 0.5$. We also take $a = 1$.

One of the roots q_i^2 is always negative and becomes quite large, while the other two can be real or complex, so the director and velocity profile through the slab is a combination of cosine and hyperbolic cosine functions.

The results for the dependence of the relaxation rate on q_x is shown in Figure 1. At small values of q_x , the relaxation rate is substantially slower than expected from the bulk expression (1) but monotonously approaches the bulk value for $q_x > 1/a$.

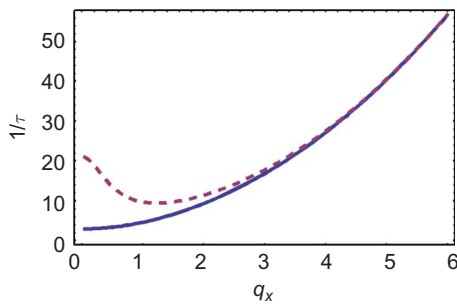


Figure 1. (colour online) The relaxation rate of the fundamental band-splay branch of fluctuations vs. q_x in homeotropic orientation. Broken line – bulk expression with $q_z = \pi/(2a)$. Units of q_x are $1/a$.

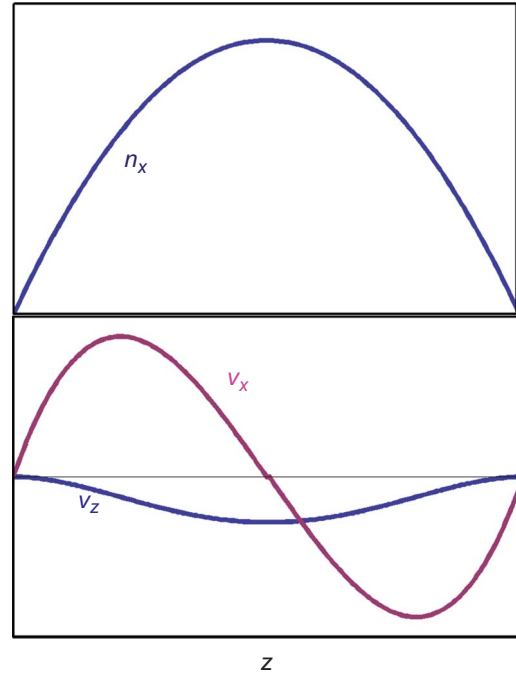


Figure 2. (colour online) Director deviation and velocity components profiles through the cell at $q_x = 0.5$. v_x remains finite at $q_x = 0$, while v_z goes to zero.

Figure 2 shows the director and velocity profile through the slab at a small value of q_x . The in-plane component of the velocity v_x decreases as q_x goes to 0, but remains finite, while v_z goes rapidly to 0.

Let us now look at the planar geometry where the fundamental mode at $q_x = 0$ is a pure splay mode. Due to the small value of α_3 , the effective viscosity in this case is nearly unaffected by the backflow and to a very good approximation equal to γ_1 . But, as q_x increases, the character of the mode becomes more bend-like and the effect of flow quenching must show up.

The linearised Ericksen–Leslie equations in this case are very similar to Equations (8), except that the fluctuating component of the director is now n_z , α_2 and α_3 are exchange roles, and instead of η_c we get η_b . We again have to solve a system of four nonlinear equations, of which one is transcendental, to get the roots q_i and the relaxation rate.

The solution for the lowest order mode exhibits an unexpected change of slope at q_x between 3 and 4. So we also calculated higher order modes by choosing for the initial estimate for the relaxation rate and for the roots appropriate values that can be guessed from the bulk expression (1) at $q_z = (2n + 1)\pi/2$. The dispersion relations for the even modes of order 1 to 3 are presented in Figure 3. The striking features are the obvious avoided crossings of the dispersion curves. We can understand them by looking at the curves that

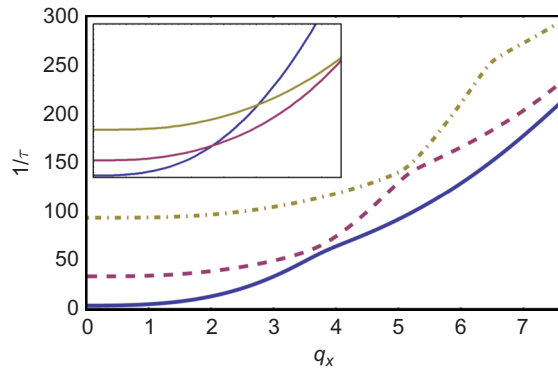


Figure 3. (colour online) Dispersion curves for the first three even splay-bend modes in the planar orientation. The inset shows the prediction of the bulk expression with crossings of the dispersion curves.

are obtained by using Equation (1) with $q_z = (2n + 1)\pi/2$. The effective viscosity decreases as the direction of the wave-vector approaches the unperturbed director, and at a given value of q_x this happens sooner for smaller values of q_z , resulting in the crossings of the dispersion curves. The boundary conditions $v(a) = 0$ perturb the bulk solution so that the degeneracy of the relaxation rate at the crossing points is removed and the crossings are avoided. This is similar to the removal of degeneracy of dispersion relations in quantum mechanics by perturbations, with the difference that the perturbation in our case is due to boundary conditions.

The change in the nature of the modes around the crossing points can be seen in Figure 4, where we plot n_z and velocity profiles for the lowest mode at values of q_x below and above the first crossing point. We see that the profile of n_z changes from having no nodes to two nodes characteristic of the $n = 2$ unperturbed mode. To be noted too is the behaviour of the velocity close to the boundary where for q_x above the crossing, v_x approaches zero in a rather thin layer. In a real sample with thickness of a few micrometres, this layer would be of the order of 100 nm or even less. It should be stressed that this is still a completely hydrodynamic result with the usual non-slip boundary condition. It is the manifestation of the fact that one characteristic root for q is imaginary and large so that the approach to zero is described by hyperbolic cosine. Correspondingly, the second-order mode crosses over from two nodes to no nodes.

The odd modes behave very similarly. There the solutions are of the form $\sin q_i z$, with the corresponding change in the determinant Equation (17). We also obtain that the degeneracy at the crossings of the odd modes is removed so that they do not cross. The odd

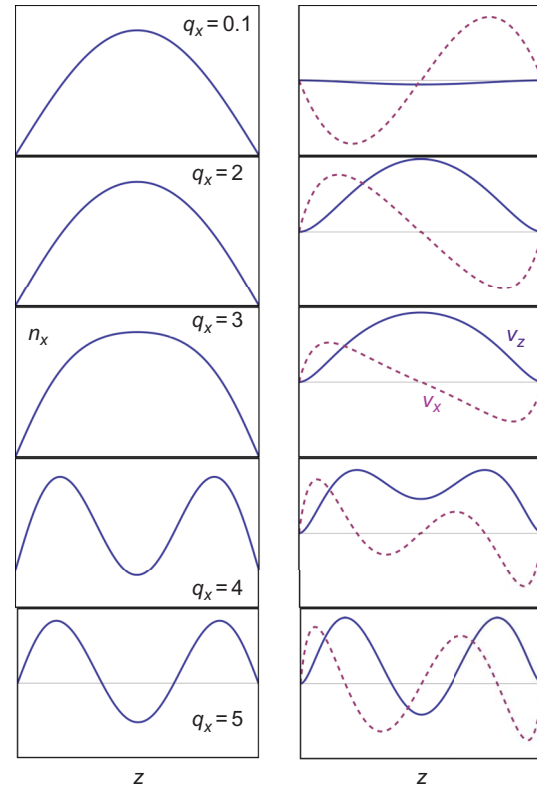


Figure 4. (colour online) Director deviation profiles and velocity profiles of the fundamental mode for values of q_x below and above first crossing point, showing the crossover from no nodes to two nodes in $n_z(z)$. Note the steep approach of v_x to zero at $z = a$ for large value of q_x .

and even modes do not mix, so they still cross, as one expects on grounds of symmetry.

The properties of the modes are important for experimental observation by light scattering. In such experiments, the wave-vector components of the observed fluctuation modes are determined by the choice of the scattering angle and light polarisation through birefringence. In samples of finite thickness, the selected q_z have a finite spread of the order of $1/a$, so mode selection cannot be perfect. In our case, the transverse profile of the modes is not a single cosine (for even modes, sine for odd), but still the mode that contribute most to the scattering signal will be the one with the biggest Fourier component, closest to the z component of the scattering vector. If this is fixed and only the x component is changed, above the crossings, the next order mode will dominate the scattering signal. In the vicinity of the crossings, both modes contribute and as the relaxation rates are close, it would be more or less impossible to separate them. So, in a realistic experimental situation, an average of several modes will be observed.

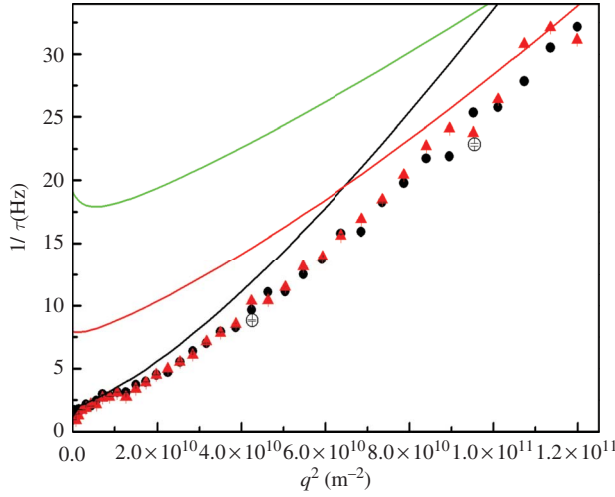


Figure 5. (colour online) Relaxation rate of 5CB obtained by dynamic difference microscopy and light scattering at room temperature. Sample thickness is 20 nm. Open circles are light scattering data. Full lines are bulk prediction for the mode dispersion using known values of the parameters of 5CB.

Figure 5 shows the results of light scattering and dynamic differential microscopy (DDM) [24] on a sample of 5CB, for which the elastic and viscosity parameters are known. In DDM, the 2D Fourier transform of the difference of successive polarised microscope images gives a time sequence of director fluctuations at a given wave-vector, from which the correlation function with corresponding relaxation rate can be calculated. The method works very well for small wave-vectors and slow relaxation rates. Its primary limitation is the speed of the camera, while the largest wave-vector is given by the pixel size. Its substantial advantage is that it is a multichannel method, giving all the modes with attainable relaxation rates and wave-vectors simultaneously. So, it complements well the standard dynamic light scattering where it is difficult to observe very low q and slow modes. The obtained data are in reasonable agreement with the theory.

Until now we have assumed strong anchoring. For finite anchoring strength, the boundary condition for the director becomes

$$K_i \left. \frac{\partial n_\alpha}{\partial z} \right|_{z=\pm a} = \pm W \quad (18)$$

where $i = 1$ and $\alpha = z$ for planar anchoring and splay-bend mode, and $i = 3$ and $\alpha = x$ for homeotropic anchoring and bend-splay mode. W is the anchoring energy. For $q_x = 0$ the interesting case is homeotropic anchoring where the mode is pure bend. Equations (10) and (11) are still valid and using

boundary condition (18), we get that q must satisfy the following transcendental equation

$$\left(q\lambda + \frac{\beta}{qa} \right) \tan qa = 1 \quad (19)$$

where $\lambda = K_3/W$ is the extrapolation length. A rather good approximate solution gives

$$\tau = \frac{a^2 \gamma_1}{3K_3} + \frac{\gamma_1 a}{W} \quad (20)$$

This is the same approximation that was obtained by completely neglecting the coupling of the director rotation and flow.

In the case of planar geometry, it is interesting to see the behaviour of the dispersion relations in the vicinity of the mixing points. The numerical calculation proceeds as in the case of strong anchoring. The calculated dispersion curves are shown in Figure 6. The lowest order mode relaxation rate is considerably slower than in the case of strong anchoring, as expected, and the mixing of the first and second mode is not apparent any more. But, the director and velocity profiles, shown in Figure 7, show that the character of the fundamental mode still changes from having no nodes at small q_x to two nodes at larger values of q_x . There v_x again goes to zero in a rather thin surface layer.

The last question we want to address is the behaviour of the fluctuations in an external field aligned parallel with the director. Let us consider the homeotropic case. We have to add to the right side of

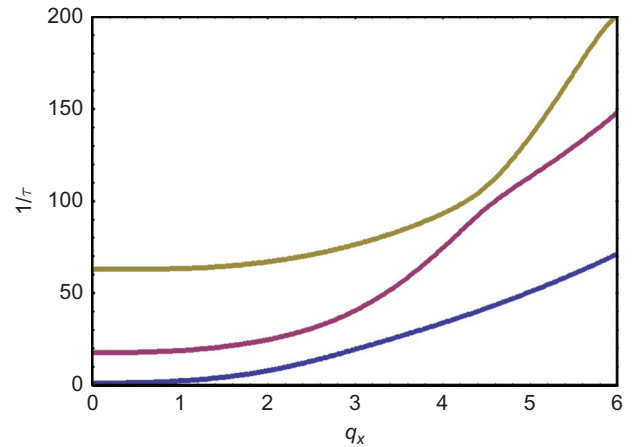


Figure 6. (colour online) Dispersion curves for the first three even modes at finite anchoring for value of $\lambda = a$. The fundamental branch is everywhere considerably below the second one.

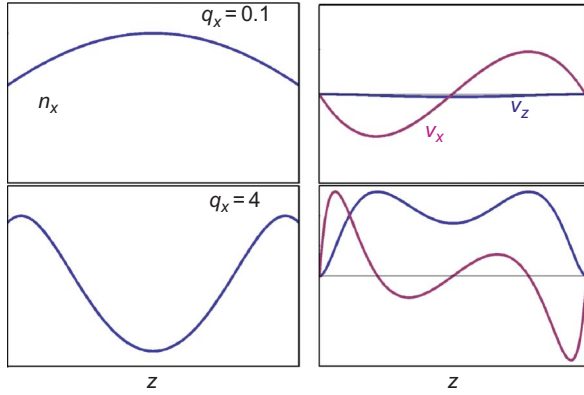


Figure 7. (colour online) Director deviation profiles and velocity profiles of the fundamental mode for values of q_x below and above first crossing point at finite anchoring with $\lambda = a$, showing the crossover from no nodes to two nodes in $n_z(z)$.

the Equation (8a) a term of the form $\varepsilon_a \varepsilon_0 E^2 n_x$. In the bulk case, this gives the well-known expression

$$\frac{1}{\tau} = \frac{K_i q_i^2 + \varepsilon_0 \varepsilon_a E^2}{\eta_{eff}} \quad (21)$$

with the same form of the effective viscosity as in the absence of the field. In our case of the slab, we can again find a good approximate solution for $q_x = 0$. Now, the relaxation rate is given by

$$\frac{\gamma_1}{\tau} (1 - \beta) = K_3 q^2 + e \quad (22)$$

where $e = \varepsilon_a \varepsilon_0 E^2$. From equations similar to (10) and the boundary conditions we get that q must satisfy

$$qa \frac{K_3 q^2 + \beta e}{\beta (K_3 q^2 + e)} = \tan qa \quad (23)$$

A rather good approximate solution for the relaxation time is

$$\frac{1}{\tau} = \frac{5}{(6 - \beta) \gamma_1} \left(\frac{3K_3}{a^2} + \frac{6}{5} \varepsilon_0 \varepsilon_a E^2 \right) \quad (24)$$

Equation (24) is accurate to within a few per cent up to fields for which $\varepsilon_0 \varepsilon_a E^2 = 10K_3/a^2$. It is to be noted that the effective viscosity for the field contribution is slightly different from the one for the elastic part of the relaxation rate.

When $q_x \neq 0$, numerical calculation shows that the dependence of the relaxation time on E^2 is still nearly exactly linear with an effective viscosity that is slightly different than for the elastic contribution. As in field-free case in Figure 1 it approaches the bulk value for $q_x > 1/a$.

4. Conclusions

For the fundamental fluctuation mode in a slab, the backflow contribution to the effective viscosity is strongly reduced so that the effective viscosity is close to the pure rotational viscosity γ_1 , as expected. For the pure bend mode in homeotropic orientation, the remaining contribution of backflow is at most about 17%. With increasing transverse wave-number q_x the relaxation rate approaches the value given by the bulk expression. The dispersion curves for the modes in planar geometry show crossing avoidance – removal of crossings and accompanying degeneracy implied by the bulk expression. The present analysis shows that in light scattering experiments for obtaining the anchoring parameters, one can assume an effective viscosity independent of the thickness of the sample and use the simple expression (5), provided that $q_x a$ is kept constant. This is best achieved by choosing $q_x = 0$. The dependence of the relaxation rate on applied field is proportional to E^2 , as in bulk, with an effective viscosity which in homeotropic orientation is slightly different from the one governing the elastic part.

Acknowledgements

The authors acknowledge the support from Slovenian Research Agency Grant No. P1-0192. M.Č. and also thanks the Isaac Newton Institute, Cambridge, for the support during the preparation of this work.

References

- [1] Durand G, Leger L, Rondelez F, Veysie M. Quasielastic Rayleigh scattering in nematic liquid crystals. *Phys Rev Lett.* 1969;22:1361–1363.
- [2] Chen GP, Takezoe H, Fukuda A. Determination of K_i ($i = 1-3$) and π_j ($j = 2-6$) in 5CB by observing the angular dependence of Rayleigh line spectral widths. *Liq Cryst.* 1989;5:341–347.
- [3] Hasegawa M, Miyachi K, Fukuda A. Accuracy of nematic viscoelastic constant measurement using Rayleigh scattered light. *J Appl Phys.* 1995;34:5694–5699.
- [4] Majumdar M, Salamon P, Jakli A, Gleeson JT, Sprunt S. Elastic constants and orientational viscosities of a bent-core nematic liquid crystal. *Phys Rev E.* 2011;83:031701-1–031701-8.
- [5] Rapini A, Papoular M. Distorsion d'une lamelle nématique sous champ magnétique. Conditions d'ancrage aux parois [Distortion of a nematic slab in magnetic field. Anchoring conditions at the walls]. *J Phys (Paris) Colloque.* 1968;30(Supp C4):54–56. French.
- [6] Park CS, Čopič M, Mahmood R, Clark NA. Dynamic behavior at a nematic liquid-crystal rubbed nylon interface using evanescent-wave photon-correlation spectroscopy. *Liq Cryst.* 1994;16:135–142.
- [7] Čopič M, Clark NA. Theory of orientational modes at nematic solid interface: when do surface-modes appear. *Liq Cryst.* 1994;17:149–155.

- [8] Stallinga S, Wittebrood MM, Luijendijk DH, Rasing T. Theory of light scattering by thin nematic liquid crystal films. *Phys Rev E*. 1996;53:6085–6092.
- [9] Wittebrood MM, Rasing T, Stallinga S, Mušević I. Confinement effects on the collective excitations in thin nematic films. *Phys Rev Lett*. 1998;80:1232–1235.
- [10] Vilfan M, Čopič M. Comparison of dynamic and static measurements of surface anchoring energy in nematic liquid crystals. *Mol Cryst Liq Cryst*. 2000;351:419–426.
- [11] Mertelj A, Čopič M. Dynamic light scattering as a probe of orientational dynamics in confined liquid crystals. *Phys Rev E*. 2000;61:1622–1628.
- [12] Vilfan M, Olenik ID, Mertelj A, Čopič M. Aging of surface anchoring and surface viscosity of a nematic liquid crystal on photoaligning poly-(vinyl-cinnamate). *Phys Rev E*. 2001;63:061709-1–061709-5.
- [13] Vilfan M, Mertelj A, Čopič M. Dynamic light scattering measurements of azimuthal and zenithal anchoring of nematic liquid crystals. *Phys Rev E*. 2002;65:041712-1–041712-7.
- [14] Vilfan M, Čopič M. Azimuthal and zenithal anchoring of nematic liquid crystals. *Phys Rev E*. 2003;68:031704-1–031704-5.
- [15] Mertelj A, Čopič M. Surface-dominated orientational dynamics and surface viscosity in confined liquid crystals. *Phys Rev Lett*. 1998;81:5844–5847.
- [16] Škarabot M, Osmanagić E, Mušević I. Surface anchoring of nematic liquid crystal 8OCB on a DMOAP-silanated glass surface. *Liq Cryst*. 2006;33:581–585.
- [17] Ericksen JL. Anisotropic fluids. *Arch Ration Mech Analysis*. 1960;4:231–237.
- [18] Ericksen JL. Inequalities in liquid crystal theory. *Phys Fluids*. 1966;9:1205.
- [19] Leslie FM. Some constitutive equations for anisotropic fluids. *Quart J Mech Appl Math*. 1966;19:357.
- [20] Leslie FM. Some constitutive equations for liquid crystals. *Arch Ration Mech Analysis*. 1968;28:265.
- [21] Knepe H, Schneider F, Sharma NK. Rotational viscosity – γ_1 of nematic liquid crystals. *J Chem Phys*. 1982;77:3203–3208.
- [22] Patricio P, Leal CR, Pinto LF, Boto A, Cidade MT. Electro-rheology study of a series of liquid crystal cyanobiphenyls: experimental and theoretical treatment. *Liq Cryst*. 2012;39:25–37.
- [23] Parodi O. Stress tensor for a nematic liquid crystal. *J Phys (Paris)*. 1970;31:581.
- [24] Giavazzi F, Brogioli D, Trappe V, Bellini T, Cerbino R. Scattering information obtained by optical microscopy: differential dynamic microscopy and beyond. *Phys Rev E*. 2009;80:031403-1–031403-15.